Mon. Not. R. astr. Soc. (1990) **243,** 151–158

CCD photometry of the distant southern globular cluster NGC 5824

R. D. Cannon,[1] Ram Sagar[1,2] and M. R. S. Hawkins[3]
[1] *Anglo-Australian Observatory, PO Box 296, Epping NSW 2121, Australia*
[2] *Indian Institute of Astrophysics, Bangalore 560034, India*
[3] *Royal Observatory, Blackford Hill, Edinburgh EH9 3HJ*

Accepted 1989 September 1. Received 1989 August 25; in original form 1989 June 29

SUMMARY

CCD observations have been used to generate a $V,(B-V)$ colour–magnitude diagram for the distant globular cluster NGC 5824. The sample consists of 285 stars reaching $V=20.5$, and a well-defined blue horizontal branch is observed for the first time. Assuming a reddening of $E(B-V)=0.13$, the colour of the giant branch at the level of the horizontal branch is determined to be $(B-V)_{o,g}=0.77$ and the apparent distance modulus $(V-M_v)=18.0\pm0.2$. From these, a value of [Fe/H] $=-1.7$ and a heliocentric distance of 33 (±3) kpc have been estimated for the cluster. This yields a galactocentric distance of 25 kpc which, when combined with Hesser, Shawl & Meyer's recent radial-velocity determination, enables the representative point of the cluster to be plotted in Lynden-Bell's velocity–distance diagram where its location is consistent with a conventional value of the mass of our Galaxy.

1 INTRODUCTION

The colour–magnitude diagram (CMD) of a globular cluster is an important tool for obtaining fundamental information about the cluster, such as its distance and chemical composition, as well as a test-bed for the study of stellar evolution. The distances and velocities of clusters give information on the structure and evolution of our Galaxy. One of the most important features in a globular cluster CMD is the horizontal branch (HB), since it can be used to estimate the cluster distance and its morphology is one of the basic classification parameters. The introduction of CCD detectors makes precise observations possible down to $V\sim20$ with moderate size telescopes, well below the HB in all but the most distant galactic clusters. In the present work, a CMD of NGC 5824 has been obtained down to $V=20.5$. This cluster was initially selected for study because it appeared to be sufficiently distant that it might contribute usefully to setting a limit on the mass of the Galaxy.

In visual appearance, NGC 5824 ≡ C1500 − 328 ($l=332\overset{\circ}{.}6$, $b=22\overset{\circ}{.}1$) is a small but rich stellar system with strong central concentration (Shapley class I), and is evidently a rather distant globular cluster. Kinman (1959) obtained an integrated spectral type of F5 for the cluster while Rosino (1961) discovered 27 variable stars, most of which are RR Lyrae variables. Harris (1975) presented the first CMD for NGC 5824 on the basis of *BV* photographic photometry, which indicated a well-defined giant branch and possibly a group of HB stars located near the plate limit at $V\sim18$. He pointed out that the cluster belongs to the moderately low-metallicity group similar to M13. Based on this CMD, Harris & Racine (1979) derived a reddening of $E(B-V)=0.14$ and an apparent distance modulus of $(V-M_v)=17.32$, but this distance estimate is not secure since the HB apparently occurred at $V=17.9$, right at the faint limit of the photometry. Zinn (1985) derived the same value for the reddening while Reed, Hesser & Shawl (1988), using new observations of the integrated colours and spectral type of the cluster, have estimated a value of 0.13 for $E(B-V)$. Chun & Freeman (1979) studied the cluster photoelectrically for radial variations of integrated *UBV* colours and found them to be uniform within a few hundredths of a magnitude. Hanes & Brodie (1985) performed *UBVRI* multi-aperture photometry for the cluster and also observed no colour gradients within the cluster. On the basis of integrated spectra, the radial velocity of the cluster has been estimated as -58 ± 16, -28 ± 13 and -38 ± 5 km s^{-1}, respectively by Mayall (1946), Zinn & West (1984) and Hesser, Shawl & Meyer (1986). For the metallicity, Zinn & West (1984) gave [Fe/H] $=-1.87\pm0.15$, while the spectral type of F4 found by Hesser *et al.* (1986) suggests [Fe/H] $=-1.98$ on the same scale.

The most distant galactic globular clusters can be used together with the dwarf spheroidal galaxies to set a lower limit on the total mass of our Galaxy (*cf.* Hartwick & Sargent 1978; Lynden-Bell, Cannon & Godwin 1983; Peterson & Latham 1989 and references therein). A better measurement of the distance to NGC 5824 was badly needed to enable it to be used in this determination. The present work provides such an estimate by locating HB stars precisely in the $V,(B-V)$ CMD.

2 OBSERVATIONS

The observations were carried out between 1984 July 24 and 28 in the *B* and *V* bands, using an RCA SID 53612 thinned black-illuminated CCD detector at the *f*/18 Cassegrain focus of the SAAO 1.0-metre telescope. At the Cassegrain focus a pixel of the 320 X 512 size CCD corresponds to 0.4 arcsec on the sky; Walker (1984) has described the instrumental setup and the filters. All exposures were pre-flashed to improve the charge-transfer efficiency. The nights were of good photometric quality, with excellent seeing (~ 1 arcsec) except on 1984 July 27/28 when it was ~ 2 arcsec. Flat-field exposures ranging from 1 to 5 s in each filter were made of the twilight sky. Six short graded exposures ranging from 1 to 30 s in *V* and seven ranging from 10 to 100 s in *B* were taken of a region that is located in the outer part of the cluster and centred on stars L, N, R and S observed photoelectrically by Harris (1975). These, in combination with the observations of two E-region standards – E8 Q3 and E9 Q1 (*cf.* Menzies, Banfield & Laing 1980), were observed for calibration purposes. The CCD observations used for the construction of the CMD are of a field offset ~ 3 arcmin to the north of the cluster so that the nucleus lies near one edge, thus maximizing the number of measurable cluster members and minimizing the proportion of field stars included in the CMD. For this purpose, five graded exposures in each pass-band were taken. They range from 100 to 6000 s in *B* and from 30 to 2000 s in *V*.

3 REDUCTIONS

The data were reduced on the Royal Observatory, Edinburgh VAX 11/780 computer using STARLINK software written by A. J. Penny. All CCD frames were cleaned of cosmic rays in the way described by Walker (1984). The flat-field and pre-flash frames were then summed after they had been normalized. This reduces the addition of extra noise in the data frames when they are corrected for pre-flashing and flat-fielded, which will ultimately improve the accuracy of the magnitude estimation of faint stars. The CCD detector is free from blemishes with only one slightly defective column, and has good evenness of response both overall and pixel-to-pixel (*cf.* Walker *et al.* 1985), enabling data frames to be flattened to better than 0.5 per cent in *B* and *V*.

The magnitude estimation of stars on each of the data frames has been done by an iterative least-squares fitting using the standard Lorentzian profile parameters for that frame, allowing for a sloping plane background (*cf.* Penny & Dickens 1986). The sum of several bright stars in each frame was used to evaluate the coefficients of the Lorentzian profiles. The residuals of the profile fit analysis were used to reject those measures which had residuals much higher than the average for a star of that magnitude.

A single reference frame was chosen in each of the two pass-bands, and the data for the other frames combined by calculating the mean frame-to-frame magnitude difference for all well-measured stars. The reference frames were chosen in such a way that, in addition to long exposure, they had high image quality and had been observed on good photometric nights at low air mass. In averaging the CCD magnitudes, measures differing from the mean for a given star by 0.2 mag or more were rejected. Altogether, less than 10 per cent of the measurements were rejected.

Zero-points for the reference frames were determined with respect to observations of E-region standards and the photoelectric stars of Harris (1975), taking into account the differences in exposure time and atmospheric extinction. The standards cover a range in brightness and colour, with $8 \leq V \leq 15.5$ and $0.04 \leq (B-V) \leq 1.14$. The colour equations given by Walker (1984) and average values of atmospheric extinction for the site were used, because they are very stable and more accurate than could be determined from the present data. The standard deviations of the zero-points are ~ 0.02 in *B* and ~ 0.01 in *V*. The internal errors estimated from the scatter in the individual measures from different exposures are listed in Table 1 as a function of *V* magnitude.

The *X* and *Y* pixel coordinates as well as *V* and $(B-V)$ magnitudes of the stars observed in NGC 5824 are listed in Table 2, along with the number of observations in each filter

Table 1. Photometric errors as a function of brightness. σ is the standard deviation per observation based on N stars.

V (mag)	σ (V) (mag)	σ (B–V) (mag)	N
15.0 – 17.0	0.015	0.018	20
17.0 – 18.0	0.030	0.044	36
18.0 – 18.5	0.033	0.048	39
18.5 – 19.0	0.035	0.046	66
19.0 – 20.0	0.040	0.061	69
20.0 – 21.0	0.050	0.066	55

Table 2. Relative positions and CCD *BV* magnitudes of stars measured in the field of NGC 5824. The number of observations and internal errors for stars in the *V* and *B* filters are denoted respectively by N_v and N_b, and σ_v and σ_b. Stars observed by Harris (1975) and Rosino (1961) have been prefixed with H and R.

Star	X (pixel)	Y (pixel)	V (mag)	(B-V) (mag)	N_v	N_b	σ_v (mag)	σ_b (mag)	Other Identifications
1	13	332	18.65	0.33	4	2	0.056	0.007	
2	14	103	16.98	0.93	3	3	0.036	0.000	
3	15	80	18.81	0.90	3	3	0.051	0.033	
4	16	352	19.00	0.86	4	3	0.051	0.031	
5	18	368	18.43	0.95	4	3	0.008	0.035	
6	18	347	19.23	1.01	2	2	0.007	0.042	
7	19	413	19.53	0.91	2	2	0.014	0.021	
8	19	340	18.20	1.03	3	2	0.033	0.014	
9	20	96	18.83	0.27	2	3	0.084	0.005	
10	20	400	18.65	0.94	3	2	0.064	0.000	
11	23	279	17.49	1.07	3	2	0.056	0.120	
12	23	328	18.81	0.16	3	2	0.014	0.035	
13	23	374	19.46	1.23	2	2	0.021	0.035	
14	24	483	20.16	0.92	3	2	0.053	0.021	
15	25	367	18.33	0.78	4	3	0.027	0.055	H56
16	29	338	18.68	0.29	3	3	0.000	0.026	
17	30	54	16.74	1.12	4	2	0.011	0.007	
18	31	35	18.82	0.37	5	3	0.045	0.029	
19	32	415	19.03	0.24	4	4	0.025	0.026	
20	32	410	19.95	0.61	2	3	0.021	0.083	
21	33	80	18.30	0.99	3	5	0.003	0.046	
22	33	328	19.00	0.82	3	3	0.022	0.067	
23	33	131	19.41	0.00	2	3	0.106	0.041	
24	35	48	18.76	0.29	2	3	0.042	0.019	
25	37	56	18.74	0.55	3	2	0.076	0.021	
26	37	347	19.00	1.05	4	3	0.031	0.057	
27	38	72	17.75	0.91	4	5	0.046	0.021	
28	40	385	19.70	0.81	4	2	0.056	0.000	

Table 2 — *continued.*

Star	X (pixel)	Y (pixel)	V (mag)	(B-V) (mag)	N_v	N_b	σ_v (mag)	σ_b (mag)	Other Identifications
29	41	365	18.31	1.07	4	3	0.043	0.014	H57
30	41	326	18.17	0.89	4	3	0.022	0.031	
31	46	340	17.74	0.79	4	2	0.042	0.014	
32	48	347	17.06	0.72	4	4	0.018	0.024	H58
33	48	408	18.64	0.69	4	4	0.029	0.007	
34	48	120	19.36	-0.19	3	3	0.050	0.031	
35	49	320	18.76	0.48	3	3	0.008	0.064	
36	50	132	18.73	0.89	3	3	0.021	0.032	
37	52	128	18.86	0.37	3	3	0.052	0.012	
38	53	451	19.82	0.90	4	3	0.042	0.060	
39	54	306	16.74	0.93	4	4	0.009	0.007	
40	54	155	18.80	0.72	2	3	0.000	0.065	
41	56	476	19.58	0.73	4	3	0.030	0.033	
42	57	279	16.95	1.09	4	5	0.007	0.017	
43	59	82	17.81	1.00	2	3	0.091	0.043	
44	59	58	18.49	0.96	2	3	0.000	0.041	
45	60	101	19.00	0.81	3	3	0.012	0.038	
46	61	287	18.62	0.31	4	4	0.036	0.015	
47	61	408	17.90	0.35	3	2	0.069	0.035	H43,R1
48	61	84	17.74	0.78	2	3	0.000	0.014	
49	62	131	18.87	-0.01	3	2	0.066	0.000	
50	62	488	18.67	0.90	3	5	0.004	0.013	H45
51	63	106	18.24	0.92	4	3	0.027	0.012	
52	63	298	15.95	1.34	4	5	0.006	0.018	
53	63	123	18.06	0.89	4	3	0.007	0.014	
54	64	75	18.30	0.90	4	4	0.032	0.030	
55	64	61	18.45	0.44	3	5	0.076	0.026	
56	66	449	19.87	0.88	4	4	0.020	0.046	
57	67	354	20.27	0.88	3	3	0.078	0.066	
58	67	291	16.16	1.20	4	3	0.004	0.003	
59	70	310	18.11	1.03	3	4	0.038	0.014	
60	71	335	18.43	0.36	4	3	0.025	0.022	
61	71	465	20.06	0.53	3	4	0.031	0.042	
62	76	482	16.95	1.65	4	4	0.017	0.009	H44
63	76	400	17.04	0.98	2	4	0.007	0.009	H42
64	76	47	18.74	0.92	4	3	0.013	0.036	
65	77	90	19.81	0.80	3	3	0.028	0.050	
66	77	361	19.34	1.30	4	4	0.029	0.043	
67	78	279	17.26	1.10	4	5	0.015	0.031	H63
68	79	250	17.97	0.93	4	4	0.037	0.028	
69	80	206	17.97	0.89	4	4	0.052	0.046	
70	81	29	20.02	0.85	3	3	0.041	0.064	
71	82	63	19.02	0.93	4	4	0.044	0.029	
72	82	97	20.25	0.00	2	3	0.000	0.017	
73	82	331	19.70	0.89	2	2	0.077	0.127	
74	82	338	19.99	1.23	2	3	0.035	0.045	
75	82	244	18.28	0.68	4	4	0.038	0.053	
76	83	126	18.58	0.95	4	3	0.054	0.037	
77	84	61	18.14	0.94	4	4	0.030	0.026	
78	85	136	18.32	0.92	4	3	0.032	0.017	
79	87	286	19.22	0.12	2	3	0.007	0.005	
80	88	383	18.63	0.26	4	3	0.020	0.045	
81	89	302	18.94	0.26	3	4	0.038	0.006	
82	90	228	18.01	1.05	3	4	0.034	0.047	
83	91	437	19.63	0.63	3	2	0.012	0.035	
84	91	312	17.49	0.86	4	5	0.020	0.035	H59
85	92	363	19.69	1.00	2	3	0.063	0.015	
86	94	150	17.76	0.92	3	2	0.026	0.007	
87	94	490	20.08	0.65	4	2	0.053	0.049	
88	95	134	19.02	0.79	3	3	0.050	0.019	
89	95	377	18.65	0.27	3	3	0.012	0.014	H41
90	96	204	18.09	1.08	4	3	0.049	0.007	
91	97	358	19.78	1.08	2	2	0.084	0.014	
92	98	334	20.38	0.83	3	2	0.047	0.014	
93	100	201	18.04	1.04	4	3	0.053	0.045	
94	100	86	18.51	0.89	3	3	0.009	0.053	
95	101	94	19.14	1.12	3	3	0.052	0.041	
96	101	269	18.91	0.86	4	3	0.015	0.012	
97	101	456	19.59	0.83	3	3	0.037	0.011	
98	102	155	19.03	0.16	3	3	0.023	0.003	
99	105	240	17.17	1.10	4	5	0.023	0.029	H62
100	106	76	20.37	1.00	2	3	0.000	0.041	
101	107	227	17.52	1.00	4	4	0.038	0.040	H61
102	108	334	16.67	1.16	5	3	0.011	0.008	H40
103	110	380	19.64	1.09	3	2	0.016	0.120	
104	111	151	18.69	0.84	3	4	0.025	0.054	
105	111	208	17.66	1.06	4	3	0.023	0.021	H238
106	112	391	20.29	0.55	2	3	0.084	0.045	
107	112	162	17.72	0.41	3	4	0.054	0.052	R14
108	114	95	18.63	0.30	4	4	0.020	0.032	
109	115	107	19.94	0.70	2	3	0.056	0.054	
110	115	125	19.70	0.72	3	4	0.066	0.043	
111	116	324	18.55	0.89	3	4	0.007	0.030	
112	116	340	18.68	0.25	5	4	0.013	0.019	H39
113	118	224	17.83	0.98	5	4	0.035	0.058	H60
114	119	350	19.22	0.97	4	4	0.020	0.049	
115	120	49	19.78	0.86	4	2	0.033	0.063	
116	120	448	19.25	0.87	3	2	0.020	0.028	
117	122	189	18.40	1.12	4	3	0.029	0.044	
118	123	118	18.16	1.05	3	3	0.049	0.044	H232
119	123	282	18.47	0.34	4	4	0.028	0.029	
120	124	495	20.60	0.79	2	3	0.021	0.039	
121	127	199	17.83	0.74	4	3	0.003	0.064	H239
122	128	269	18.16	0.99	4	4	0.032	0.043	
123	128	469	17.51	1.08	5	5	0.018	0.012	H23
124	128	341	18.40	0.04	4	5	0.004	0.023	
125	129	235	17.69	0.97	5	3	0.023	0.005	
126	129	458	20.28	0.88	3	3	0.033	0.057	
127	130	191	17.21	1.11	4	5	0.006	0.023	H237
128	132	407	20.08	1.40	3	2	0.031	0.056	
129	133	207	17.78	0.91	4	4	0.007	0.017	H240
130	134	160	19.39	0.17	3	4	0.024	0.006	
131	135	230	17.95	1.00	4	2	0.017	0.000	
132	136	370	20.28	0.84	3	3	0.033	0.043	
133	136	412	20.90	0.09	2	4	0.049	0.020	
134	137	170	16.91	1.12	5	5	0.016	0.018	H235
135	137	135	16.70	1.18	4	5	0.004	0.013	H233
136	137	456	18.83	0.22	2	4	0.000	0.038	
137	137	319	19.77	0.70	2	4	0.049	0.052	
138	138	281	19.28	0.19	4	4	0.045	0.048	
139	139	467	18.61	0.30	4	2	0.015	0.007	
140	140	98	19.81	0.77	4	4	0.025	0.054	
141	142	486	20.52	0.75	3	2	0.041	0.021	
142	144	444	17.00	1.05	5	4	0.043	0.017	H24
143	144	454	19.45	1.12	3	2	0.033	0.071	
144	146	185	16.00	1.34	4	5	0.013	0.006	H236
145	146	354	19.95	0.69	4	3	0.029	0.041	
146	148	113	17.46	1.04	4	4	0.008	0.007	H231
147	148	169	18.98	0.74	4	5	0.004	0.032	
148	149	229	16.49	1.18	5	5	0.028	0.006	H35
149	149	247	20.17	0.67	2	3	0.007	0.021	
150	149	297	19.56	0.09	3	3	0.012	0.024	
151	149	269	20.60	0.82	2	2	0.000	0.035	
152	150	145	19.47	0.65	4	3	0.051	0.067	
153	150	105	19.96	0.99	3	3	0.045	0.057	
154	151	383	18.52	0.31	5	5	0.019	0.005	
155	151	96	20.23	0.91	3	2	0.056	0.021	
156	151	285	19.87	0.76	3	2	0.062	0.077	
157	152	485	17.59	1.03	5	4	0.024	0.023	H22
158	153	471	20.99	0.44	2	2	0.000	0.021	
159	154	438	17.81	1.51	4	3	0.020	0.007	H25
160	154	34	19.65	0.89	3	2	0.078	0.028	
161	154	261	18.78	0.16	3	5	0.009	0.043	
162	154	124	17.15	1.07	4	4	0.003	0.009	H234
163	155	141	20.19	0.29	3	2	0.078	0.000	
164	156	76	18.24	1.05	4	4	0.046	0.039	H230
165	157	336	16.59	1.16	5	4	0.016	0.004	H30
166	161	323	20.80	0.04	2	3	0.028	0.044	
167	163	296	18.07	1.03	4	4	0.012	0.037	H32
168	163	141	20.20	1.04	3	3	0.067	0.042	
169	165	177	18.31	0.73	3	5	0.007	0.034	
170	166	149	20.25	0.76	2	3	0.028	0.064	
171	166	411	19.33	0.17	3	4	0.012	0.009	
172	167	190	18.05	0.88	5	4	0.037	0.032	
173	168	339	17.91	0.98	4	3	0.004	0.000	H29
174	168	302	18.47	0.92	5	4	0.025	0.045	H31
175	169	180	18.81	0.19	3	4	0.053	0.011	
176	170	359	18.28	0.96	4	4	0.022	0.027	H28
177	171	291	18.55	0.49	3	2	0.029	0.000	
178	171	90	18.61	0.43	2	2	0.000	0.000	H229,R21
179	172	237	18.65	0.33	3	4	0.008	0.034	H34
180	173	34	20.46	-0.08	3	3	0.072	0.021	
181	173	250	20.11	0.41	3	3	0.052	0.031	
182	175	198	18.55	1.05	4	4	0.043	0.044	
183	176	39	18.58	0.34	4	4	0.020	0.023	H229
184	176	395	19.33	0.79	3	3	0.024	0.036	
185	178	94	18.93	0.94	3	4	0.031	0.031	
186	179	218	17.15	1.11	2	4	0.007	0.037	H242
187	180	382	18.70	0.32	4	4	0.044	0.031	H26
188	181	353	19.07	0.84	3	2	0.017	0.000	H27
189	182	420	20.39	0.78	3	2	0.052	0.035	
190	182	113	18.53	0.35	5	4	0.034	0.004	
191	184	481	20.16	0.80	4	2	0.048	0.021	
192	185	240	18.35	0.95	3	3	0.007	0.061	H33

Table 2 — *continued.*

Star	X (pixel)	Y (pixel)	V (mag)	(B-V) (mag)	N_v	N_b	σ_v (mag)	σ_b (mag)	Other Identifications
193	186	230	19.16	0.41	3	2	0.017	0.014	
194	186	201	18.77	0.24	3	5	0.019	0.024	
195	188	328	18.89	0.87	2	4	0.084	0.026	
196	188	263	19.90	0.62	3	2	0.020	0.110	
197	189	221	19.34	0.96	2	2	0.021	0.014	
198	189	369	18.47	0.98	3	3	0.029	0.054	
199	190	472	19.96	0.82	4	2	0.038	0.000	
200	192	156	19.12	1.14	3	4	0.029	0.034	
201	192	313	19.14	0.87	3	4	0.016	0.048	
202	193	507	18.67	1.16	3	2	0.062	0.007	
203	193	254	18.99	0.16	4	3	0.022	0.016	
204	194	59	18.63	0.99	3	5	0.033	0.003	
205	195	271	20.03	1.13	2	3	0.042	0.031	
206	195	379	17.40	1.04	4	3	0.019	0.019	
207	197	374	16.66	1.18	4	4	0.006	0.006	
208	197	145	16.96	1.10	4	4	0.011	0.013	H243
209	198	41	20.26	0.75	3	2	0.065	0.007	
210	199	364	19.63	0.89	2	3	0.028	0.033	
211	200	54	18.60	0.30	3	3	0.036	0.007	
212	204	29	19.73	0.98	3	2	0.045	0.021	
213	205	349	17.05	1.14	5	4	0.022	0.006	H15
214	206	94	18.81	0.22	3	4	0.012	0.041	
215	207	402	20.61	0.86	2	3	0.042	0.033	
216	207	498	19.52	0.78	3	2	0.027	0.042	
217	209	89	18.81	0.97	3	3	0.024	0.009	
218	210	149	18.64	0.31	4	3	0.006	0.028	
219	210	211	20.69	0.41	3	2	0.017	0.007	
220	210	32	20.07	0.08	2	4	0.007	0.049	
221	213	282	20.11	0.99	3	2	0.059	0.084	
222	213	121	18.45	0.34	4	4	0.004	0.015	
223	214	265	17.98	0.91	4	4	0.002	0.014	
224	215	48	18.33	0.96	3	2	0.007	0.000	
225	219	343	16.44	0.97	5	4	0.003	0.009	H14
226	221	261	19.89	0.98	3	2	0.040	0.106	
227	222	357	20.38	0.68	3	2	0.017	0.035	
228	223	242	19.80	0.13	3	3	0.022	0.027	
229	225	375	18.69	0.22	3	4	0.031	0.006	
230	226	225	19.73	0.83	3	3	0.045	0.028	
231	229	417	18.74	0.27	4	4	0.031	0.011	
232	229	89	16.25	1.26	5	5	0.016	0.009	H228
233	234	167	19.71	1.13	3	2	0.062	0.064	
234	235	393	15.47	1.59	5	5	0.007	0.006	H7
235	236	301	19.78	0.64	2	2	0.007	0.057	
236	237	496	20.86	0.33	2	2	0.042	0.042	
237	238	154	17.97	0.27	4	3	0.012	0.007	
238	240	174	20.33	0.76	3	2	0.037	0.014	
239	241	66	17.61	1.04	4	4	0.014	0.009	H227
240	245	238	19.48	1.12	3	2	0.073	0.007	
241	248	91	19.50	0.89	4	4	0.045	0.046	
242	249	483	20.66	0.75	3	2	0.087	0.014	
243	250	181	18.73	1.60	4	4	0.052	0.033	
244	252	377	18.62	0.90	4	5	0.038	0.032	H8
245	254	58	20.35	0.89	3	2	0.072	0.084	
246	256	153	19.13	0.87	3	4	0.011	0.032	
247	259	231	19.88	0.90	3	3	0.040	0.012	
248	259	245	18.59	0.60	2	3	0.000	0.044	R5
249	261	316	20.47	0.42	2	2	0.021	0.035	
250	263	458	19.02	0.74	4	4	0.022	0.047	H6
251	263	417	18.70	0.19	4	5	0.025	0.011	
252	264	39	20.50	0.85	2	2	0.021	0.035	
253	265	433	18.88	0.20	4	4	0.037	0.009	
254	266	186	18.46	0.83	5	4	0.045	0.015	
255	266	308	18.09	1.07	4	4	0.006	0.052	H11
256	266	138	19.37	0.99	4	4	0.037	0.028	
257	267	67	18.87	0.19	4	3	0.020	0.009	
258	267	295	20.28	1.03	2	2	0.021	0.021	
259	267	165	18.77	0.27	4	4	0.028	0.007	
260	267	339	19.37	1.26	3	4	0.040	0.058	
261	271	205	18.70	-0.28	2	2	0.007	0.000	R2
262	272	457	20.35	0.96	2	2	0.098	0.014	
263	273	47	20.11	0.98	3	3	0.025	0.069	
264	274	81	19.59	0.81	3	4	0.040	0.024	
265	275	497	18.96	0.97	3	4	0.012	0.047	
266	275	342	18.19	0.93	4	4	0.034	0.014	H9
267	275	195	18.60	0.31	3	3	0.048	0.025	
268	275	477	15.26	0.78	5	5	0.018	0.007	H5
269	276	497	20.13	1.03	2	2	0.000	0.021	
270	278	233	21.18	0.18	2	2	0.028	0.049	
271	278	218	18.79	0.22	4	5	0.041	0.029	
272	280	237	19.43	0.20	4	3	0.038	0.009	
273	285	42	16.67	0.78	4	5	0.015	0.000	H248

Table 2 — *continued.*

Star	X (pixel)	Y (pixel)	V (mag)	(B-V) (mag)	N_v	N_b	σ_v (mag)	σ_b (mag)	Other Identifications
274	287	211	20.49	0.89	3	2	0.050	0.007	
275	287	245	18.51	0.92	4	5	0.028	0.016	
276	288	126	20.49	1.09	2	2	0.035	0.099	
277	289	108	20.52	0.83	3	2	0.054	0.000	
278	289	70	20.28	0.99	3	3	0.040	0.067	
279	291	277	20.25	0.90	3	3	0.071	0.057	
280	292	324	18.03	0.86	4	5	0.051	0.029	H10
281	293	61	20.39	0.75	3	2	0.076	0.021	
282	301	133	19.05	0.98	3	4	0.054	0.041	
283	302	55	20.68	0.50	3	3	0.040	0.012	
284	311	292	20.42	0.69	2	3	0.077	0.077	
285	316	333	20.04	1.15	4	2	0.045	0.042	

and the standard deviations estimated from the agreement between the measures of each star. Only stars with at least two measures in each filter are included in Table 2 and used in the subsequent analysis. One consequence of the procedure for rejecting discrepant measures is that the mean magnitudes of the known RR Lyrae variable stars (Rosino 1961) are somewhat meaningless, but they are included in Table 2 for completeness and can be identified by the prefix 'R' in the final column. An identification map for the stars is shown in Fig. 1. The X and Y pixel coordinates can be transformed into relative α and δ positions using the following relations

$$\Delta\alpha = 126.81 + 0.0082 \times X - 0.4618 \times Y$$

$$\Delta\delta = -83.82 + 0.3913 \times X + 0.0110 \times Y,$$

where $\Delta\alpha$ and $\Delta\delta$ are the differences in arcsec relative to $\alpha = 15^h00^m52\overset{s}{.}0$, $\delta = -32°51'00''$ (1950). These transformations have been determined by astrometric measurements relative to a set of Perth 70 and SAO stars, on a film copy of the SERC(J) plate of field 387 in the ESO/SERC Southern Sky Survey, and are accurate to within 1 arcsec.

To compare the present CCD photometry with the photographic data of Harris (1975), the differences in the sense photographic minus CCD are plotted in Fig. 2 and the statistical results of the same are listed in Table 3. These show that

(i) on average, the present $(B-V)$ values are 0.1 redder than the ones given by Harris (1975), except for faint and blue stars [i.e. $V > 18.5$ and $(B-V) < 0.4$] located near the limit of the photographic observations. There may be a small systematic trend with colour but this cannot be unambiguously determined.

(ii) The CCD V magnitudes for stars brighter than $V = 17$ (the limiting magnitude of the photoelectrically observed stars used by Harris 1975) are about 0.1 fainter than the photographic V magnitudes. This difference increases rapidly for fainter stars, for which Harris extended his photoelectric sequence using an auxiliary 'calibration lens'.

These discrepancies are clearly systematic and are much larger than the random internal errors of the CCD data. The errors are more likely to lie in the photographic observations for the following reasons:

(i) the CCD, unlike the photographic plate, is an intrinsically linear detector.

(ii) the CCD camera has a larger plate scale (≈ 11.46 arcsec mm^{-1}) than the photographic plates (≈ 22.54 arcsec

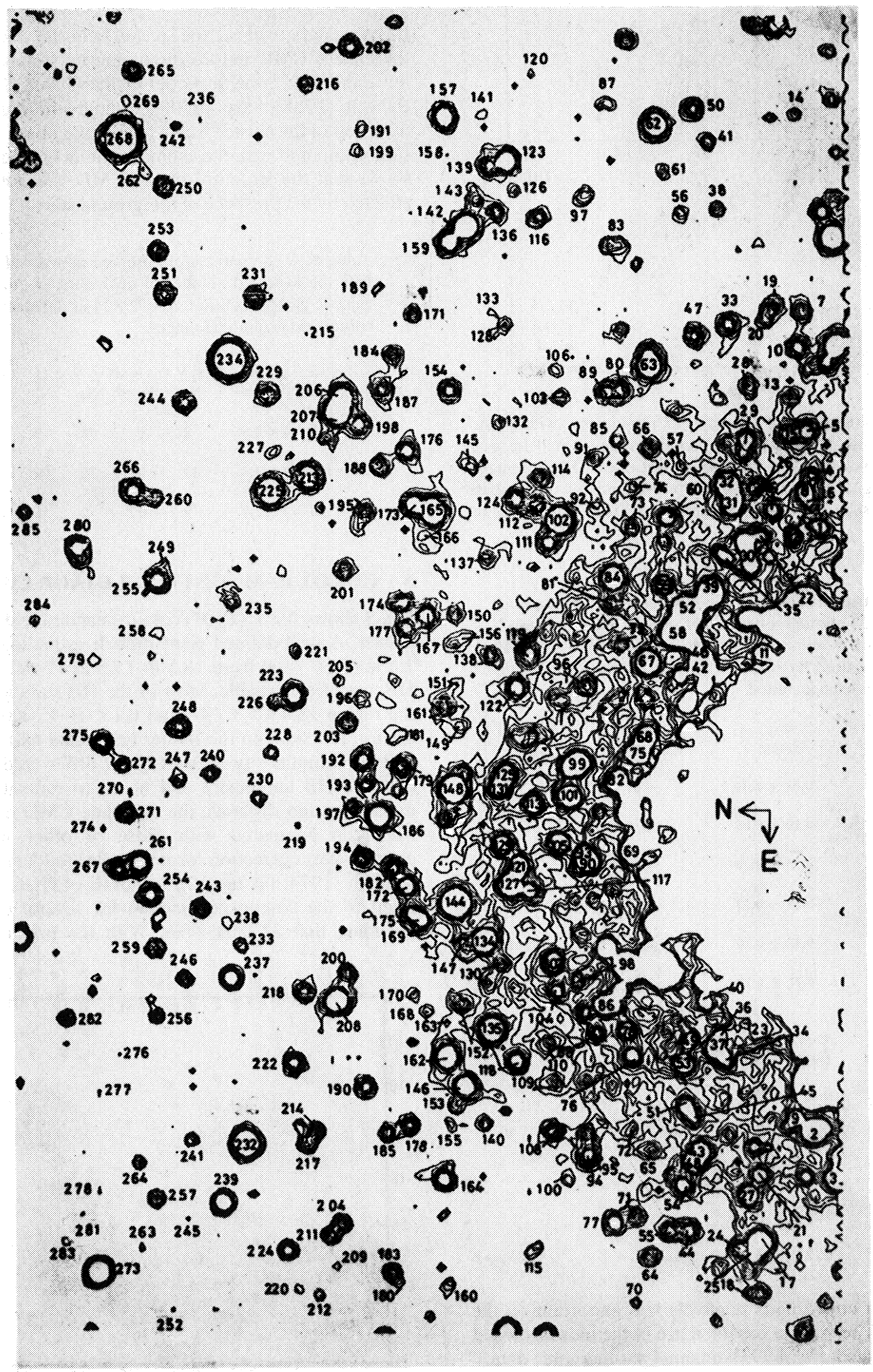

Figure 1. Identification map for measured stars. The map is a contour plot of a CCD frame in *V* with 1000 s exposure. East is towards the bottom and north is to the left, and the frame size is ~ 128 by 205 arcsec.

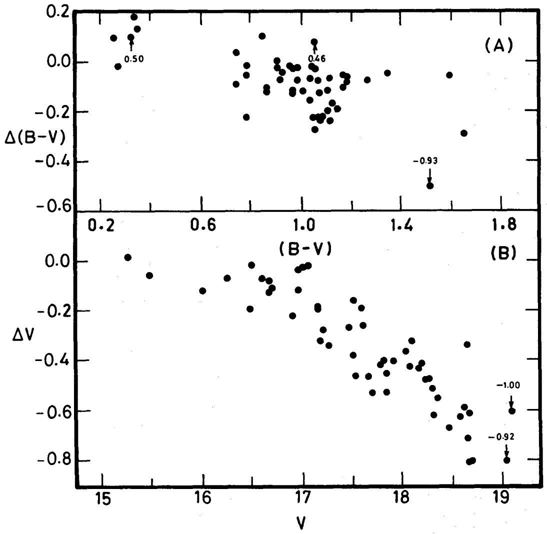

Figure 2. A comparison of the present photometry with photographic data given by Harris (1975). The differences are in the sense photographic minus present, plotted against the CCD photometry. Numbers in Fig. 2 denote values of the ordinates of those points whose positions lie outside the diagram, in the directions of the arrows.

Table 3. Statistical results of the differences Δ in the sense Harris' (1975) photographic minus present CCD values. V and $(B-V)$ are from present photometry. The errors are the standard deviations based on N stars. A few very discrepant stars have not been included.

V (mag)	$\sigma_{\Delta V}$ (mag)	$\sigma_{\Delta(B-V)}$ (mag)	N
15.5 – 16.5	−0.08 ± 0.07	−0.07 ± 0.02	6
16.5 – 17.0	−0.10 ± 0.06	−0.10 ± 0.05	8
17.0 – 17.5	−0.25 ± 0.10	−0.15 ± 0.07	8
17.5 – 18.0	−0.39 ± 0.12	−0.10 ± 0.06	11
18.0 – 18.5	−0.48 ± 0.10	−0.13 ± 0.09	11
18.5 – 19.1	−0.71 ± 0.19	0.06 ± 0.07	9

(B−V) (mag)	$\sigma_{\Delta(B-V)}$ (mag)	N
0.2 – 0.4	0.09 ± 0.07	4
0.7 – 0.9	−0.05 ± 0.04	10
0.9 – 1.0	−0.07 ± 0.04	9
1.0 – 1.1	−0.15 ± 0.08	14
1.1 – 1.7	−0.12 ± 0.08	12

mm^{-1}), so that crowding is relatively less important on the CCD frames. The stars in common are in the most crowded region for which Harris (1975) obtained photographic data.

(iii) In the present analysis, the crowding problem has been tackled to some extent by using Lorentzian profile parameters; whereas Harris (1975) used simple iris photometry to measure the stars.

4 FIELD STAR CONTAMINATION

It is necessary to check the level of field star contamination in the cluster CMD before discussing its structure. Based on the Bahcall & Soneira model of the Galaxy, Ratnatunga & Bahcall (1985) have predicted field-star densities in the direction of the cluster. Table 4 gives the observed number of stars compared with the estimated number of field stars, and shows that the structure of the CMD will not be seriously affected by the presence of foreground stars.

Table 4. A comparison of observed number of stars, N_0, with the expected number of field stars, N_e, towards the galactic globular cluster NGC 5824 in different apparent colour and magnitude ranges.

Colour range (mag)	15 ≤ V < 17 N_o	N_e	17 ≤ V < 19 N_o	N_e	19 ≤ V < 21 N_o	N_e
(B−V) ≤ 0.8	2	1	73	2	71	7
0.8 < (B−V) ≤ 1.3	19	2	72	6	43	8
(B−V) > 1.3	2	0	2	1	1	7

5 COLOUR–MAGNITUDE DIAGRAM

Fig. 3 shows the $V,(B-V)$ colour–magnitude diagram of the cluster. A well-defined giant branch extending from 0.9 to 1.6 in $(B-V)$ and from 18.5 to 15.5 in V, and a strong blue HB, are clearly visible. Most of the HB stars are situated in the region $18.4<V<19.4$ and $0.1<(B-V)<0.4$, and there are too few stars on the redder horizontal part of the HB to define its luminosity accurately. In order to determine the effective HB luminosity, and hence to estimate the cluster metallicity and distance, the complete CMD of NGC 5824 has been compared with those of other well-observed clusters after correction for interstellar reddening. Following Cannon (1974; his fig. 12), the BHB of NGC 5824 can be fitted to the composite diagram for several other clusters assuming that $M_V(\mathrm{HB})=0.6$. With the preferred value of

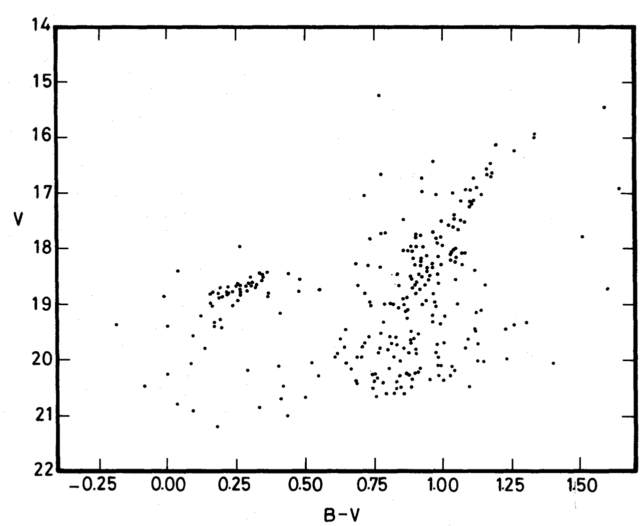

Figure 3. The $V,(B-V)$ colour–magnitude diagram of stars in NGC 5824.

$E(B-V)=0.13$, the true HB occurs at $V=18.6$ while $(B-V)_{o,g}=0.77$. NGC 5824 seems to be similar to intermediate-metallicity clusters such as NGC 6752 and M13, although the giant branch is a little steeper than in those two clusters. A slightly better fit to the whole upper CMD can be obtained if both reddening and distance are treated as free parameters, with $E(B-V)=0.22$, $V_{HB}=18.5$ and $(B-V)_{o,g}=0.69$, making NGC 5824 a typical metal-poor globular cluster, but this seems a somewhat arbitrary procedure given the rather sparsely populated red giant branch of the cluster. Therefore in what follows the distance and metallicity are estimated on the basis of the independently determined reddening, $E(B-V)=0.13$ (Reed *et al.* 1988).

6 METALLICITY

The best way to estimate the metallicity of a globular cluster is to measure lines in high-dispersion spectrograms of a few of its member stars and derive [Fe/H] via a curve of growth analysis or through comparison with synthetic spectra. Given a lack of such observations, indirect methods must be used for estimating the metallicity of NGC 5824. Zinn & West (1984) give NGC 5824 a metallicity [Fe/H] $= -1.87 \pm 0.15$, based on the Q-method which uses integrated photometry, while the Hesser *et al.* (1986) integrated spectral type implies [Fe/H] $= -1.98$. Adopting $E(B-V)=0.13$ as the cluster reddening and using Zinn & West's (1984) relation for [Fe/H] with $(B-V)_{o,g}$ yields a slightly higher metallicity of [Fe/H] $= -1.7 \pm 0.15$. It would be interesting to obtain photometry for a larger sample of faint stars to see if NGC 5824 has a populous extended hot blue HB like those of NGC 6752 and M 13 (*cf.* Cannon 1984, and references therein). The appearance of a few faint blue stars, where very few field stars are expected in Fig. 3, hints at this possibility, although some of these could alternatively be blue straggler stars, or simply poor data given that the stars are near the faint limit in a relatively crowded field.

7 DISTANCE

The apparent V magnitude for the HB is 18.6. Taking the commonly adopted value of $M_v(\mathrm{HB})=0.6$, the apparent distance modulus to the cluster $(V-M_v)$ is 18.0 ± 0.2. Alternatively, if M_v(HB) depends on metallicity according to the relation derived by Gratton (1985) and [Fe/H] $=1.7$ for the cluster, the value of M_v(HB) is 0.65, which is not significantly different. Consequently, an apparent modulus of 18.0 is adopted here for the cluster. Taking $R=3.1$ and $E(B-V)=0.13$, the true distance modulus to the cluster comes out to be 17.6 ± 0.2, which yields a distance of 33 (± 3) kpc. This corresponds to a galactocentric distance of 25 kpc (assuming the Sun to be at a galactocentric distance of 8.5 kpc), about 30 per cent greater than that derived from Harris's (1975) distance estimate.

8 IMPLICATIONS FOR THE MASS OF THE GALAXY

Lynden-Bell has shown that the radial velocities of the most distant galactic globular clusters and dwarf spheroidal galaxies can be used to set a lower limit on the total mass of the Galaxy (Lynden-Bell *et al.* 1983). According to Hesser *et al.* (1986) the heliocentric radial velocity of NGC 5824 is -38 ± 5 km s^{-1}, giving $V_{GSR} = -127$ km s^{-1} relative to the Galactic Centre. With this recent accurate velocity and the present distance estimate, the cluster can be added to Lynden-Bell's diagram (Fig. 4), where its location is indicated by an asterisk. The uncertainties in velocity and distance are such that the position of NGC 5824 in this diagram is uncertain by only about the size of the plotted symbol.

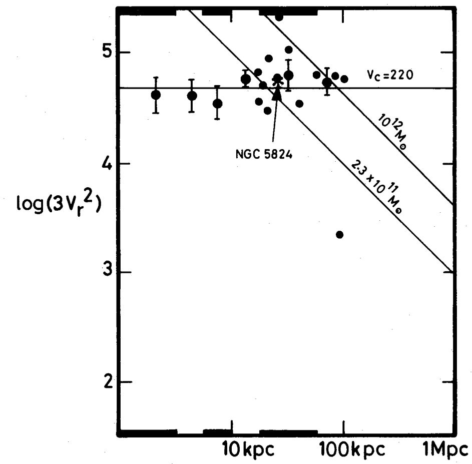

Figure 4. Lynden-Bell's velocity–distance diagram for galactic globular clusters. The distances are from the Galactic Centre and V_r are the line-of-sight velocities corrected for the solar motion with respect to the local standard of rest and for the motion $V_c = 220$ km s^{-1} of the LSR. Heavy points are means of $3V_r^2$ for globular clusters in the columns indicated in the margins. The small points are individual globular clusters in the outer part of the galaxy. The location of NGC 5824 is marked by an asterisk.

Although NGC 5824 seems to be somewhat more distant than was believed formerly, the cluster point still lies close to the line corresponding to a galactic mass of $2.3 \times 10^{11} M_\odot$. As was pointed out by Lynden-Bell *et al.* (1983), many of the high points in this diagram, which seemed to imply a very high galactic mass and hence some sort of missing mass, moved to lower mass lines (with lower velocities or smaller distances) when more accurate data were obtained. There is now one more accurately located point which is consistent with a conventional value for the mass of the Galaxy.

9 CONCLUSIONS

B, V CCD magnitudes down to $V=20.5$ are presented for 285 stars in NGC 5824. The present work leads to the following conclusions.

(i) Generally the CCD magnitudes are a little fainter and redder than the photographic data given by Harris (1975), but it appears that there are substantial systematic errors in the photographic photometry for the faintest stars near the photographic plate limit at $V \sim 18$.

(ii) The new CMD shows a well-defined red giant branch and a strong blue HB at $V \sim 18.6$; both the giant branch and perhaps a hot blue HB can be traced to the limit of the data at $V \sim 20.5$.

(iii) Adopting $E(B-V)=0.13$, the value of $(B-V)_{o,g}=0.77$ yields [Fe/H] $= -1.7$, slightly higher than other estimates.

(iv) From the morphology of the CMD, NGC 5824 seems to be a typical moderately metal-poor globular cluster.

(v) The location of the horizontal branch indicates an apparent distance modulus of $(V-M_v)=18\pm0.2$, corresponding to a distance of 33 (±3) kpc to the cluster and a galactocentric distance of 25 kpc.

(vi) In Lynden-Bell's velocity-distance diagram, the cluster representative point lies close to the line corresponding to a galactic mass of at least $2.3\times10^{11}M_\odot$.

ACKNOWLEDGMENTS

We are grateful to A. J. Penny for help and valuable suggestions during the data reduction, and to colleagues at the AAO for useful comments on a first draft of this paper. RS thanks the Nuffield Foundation, administered by the Royal Society of London, and the Royal Observatory, Edinburgh for providing financial support.

REFERENCES

Cannon, R. D., 1974. *Mon. Not. R. astr. Soc.,* **167,** 551.
Cannon, R. D., 1984. *Observational Tests of the Stellar Evolution Theory, IAU Symp. No. 105,* p. 123, eds Maeder, A. & Renzini, A., D. Reidel, Dordrecht.
Chun, M. S. & Freeman, K. C., 1979. *Astrophys. J.,* **227,** 93.
Gratton, R. G., 1985. *Astr. Astrophys.,* **147,** 169.
Hanes, D. A. & Brodie, J. P., 1985. *Mon. Not. R. astr. Soc.,* **214,** 491.
Harris, W. E., 1975. *Astrophys. J. Suppl.,* **29,** 397.
Harris, W. E. & Racine, R., 1979. *Ann. Rev. Astr. Astrophys.,* **17,** 241.
Hartwick, F. D. A. & Sargent, W. L. W., 1978. *Astrophys. J.,* **221,** 512.
Hesser, J. E., Shawl, S. J. & Meyer, J. E., 1986. *Publs astr. Soc. Pacif.,* **98,** 403.
Kinman, T. D., 1959. *Mon. Not. R. astr. Soc.,* **119,** 538.
Lynden-Bell, D., Cannon, R. D. & Godwin, P. J., 1983. *Mon. Not. R. astr. Soc.,* **204,** 87P.
Mayall, N. U., 1946. *Astrophys. J.,* **104,** 290.
Menzies, J. W., Banfield, R. M. & Laing, J. D., 1980. *S. Afr. astr. Obs. Circ.,* **1,** 149.
Penny, A. J. & Dickens, R. J., 1986. *Mon. Not. R. astr. Soc.,* **220,** 845.
Peterson, R. C. & Latham, D. W., 1989. *Astrophys. J.,* **336,** 178.
Ratnatunga, K. U. & Bahcall, J. N., 1985. *Astrophys. J. Suppl.,* **59,** 63.
Reed, B. C., Hesser, J. E. & Shawl, S. J., 1988. *Publs astr. Soc. Pacif.,* **100,** 545.
Rosino, L., 1961. *Publs astr. Soc. Pacif.,* **73,** 309.
Walker, A. R., 1984. *Mon. Not. R. astr. Soc.,* **209,** 83.
Walker, D. D., Sanford, P. E., Lyons, A., Fordham, J., Bone, D. Walker, A. R. & Boksenberg, A., 1985. *Proc. 8th Symp., Photoelectric Devices,* p. 185, ed. Morgan, B. L., Academic Press, London.
Zinn, R., 1985. *Astrophys. J.,* **293,** 424.
Zinn, R. & West, M. J., 1984. *Astrophys. J. Suppl.,* **55,** 45.